An EMG Enhanced Impedance and Force Control Framework for Telerobot Operation in Space

Ning Wang
Department of Computer Science and Engineering, The Chinese University of Hong Kong, Hong Kong
nwang@cse.cuhk.edu.hk

Chenguang Yang
School of Computing and Mathematics, Plymouth University, United Kingdom
cyang@ieee.org

Michael R. Lyu
Department of Computer Science and Engineering, The Chinese University of Hong Kong, Hong Kong
lyu@cse.cuhk.edu.hk

Zhijun Li
Key Lab of Autonomous System and Network Control, College of Automation Science and Engineering, South China University of Technology, Guangzhou, China
zjli@ieee.org

Abstract—**Tele-operation is a merging point of modern developments in robotics and communications technologies. Both traditional applications (e.g., mining) and emerging domains (e.g., microsurgery) benefit from the advancement of tele-robotic systems. Combining a local human operator and a remote autonomous robot, the tele-robotics systems could optimally exploit both the intelligence of human operator and the automation of robot. In a tele-operation scenario, the exchange of force and position signals, i.e., haptic feedback, can greatly extend human operator's capability of conducting complicated work through the robot in a remote environment. However, long-range communications usually suffer from the time delay problem caused by the inherent characteristics of communication channels. Delayed transmission of haptic signals may lead to instability in the closed-loop telerobot control system. Although much effort has been made in the control community to overcome this difficulty, and many approaches such as wave scattering, passivity, and small gain theorem have been employed as possible solutions, stability in haptic telerobot control remains a challenge. It has been noted that the neural path of human being is also subject to transmission delay as well. We know that in the presence of time delay in sensory feedback pathways, human neural control can easily maintain stability and even to show superior manipulation skills in unstable interaction scenarios. It has been discovered and reported that the operation stability of human beings could be achieved by well adjusting the mechanical impedance, i.e., the resistance to imposed motion, which is largely contributed by the spring-like property of muscles.**

Being investigated in robotics community for decades, impedance control has shown great advantage in terms of safety and flexibility over conventional position or force control. However, only until very recently our attention has been attracted to transferring a human operator's muscle impedance to a telerobot. In the current research, we aim at extracting and transferring both force and impedance information from human muscles to achieve force and impedance control of a remote robot, especially in the context of space robot application.

Over the last decades, research efforts have been made to develop humanoid robots that could assist astronauts in performing space-related tasks. A robot for this purpose is expected to be as dexterous as a suited astronaut, and at the same time is envisioned to be able to collaborate with the astronaut, either autonomously or by tele-operation. The key design philosophy of this kind of humanoid robotics is to guarantee the human and robot can interact in a human friendly manner.

In this paper we mainly focus on the study of Electromyography (EMG) signals to extract force and impedance information for control of remote telerobot. As a physiological signal generated by muscle cells, EMG reflects human muscle activations and tensions, therefore it has long been utilized and analyzed for investigation of human motor control. EMG is recently recognized as a suitable means for extracting impedance of human muscles. To this end, we propose a framework of EMG enhanced impedance and force control, in which EMG signals are captured during the interactions between the human operator and a remote robot. To extend our previous work on force estimation using EMG, this study mainly focuses on the extraction of human operator's impedance from EMG data measured at skeletal muscle positions. As the high frequency band of the EMG signals is mainly used, we employ the AM-FM decomposition technique to extract EMG signals amplitude, and then apply a linear mapping to estimate impedance. A preliminary simulated experiment is carried out to demonstrate the effectiveness of our method. More techniques will be developed in the future under this proposed framework, which are expected to contribute to both the human-robot interaction (HRI) and telerobot control, with application in aerospace-related tasks.

TABLE OF CONTENTS

1. INTRODUCTION

Robotics technologies deal with the design, construction, operation, and application of robots, as well as computer systems for their control, sensory feedback, and information processing. These technologies can be applied to tele-operation, which employs automated machines that can take the place

978-1-4799-1622-1/14/$31.00 ©2014 IEEE

of humans in various environments. Robotics technologies can also be used to assist human for improving their life quality, especially for those disabled and the elderly. Tele-operated robots, or telerobots, are usually remotely operated from a distance by a human operator, rather than following a predetermined sequence of movements. They have a large range of applications when humans cannot be present on site to perform a certain task, which especially applies to the scenario when the task site is hazardous, far away, or inaccessible by human. The telerobots are usually located away from human operators, e.g., in another room or in another country, or may be on a very different scale from the operator. For instance, a laparoscopic surgery robot allows the surgeon to work inside a human patient on a relatively small scale compared to open surgery, significantly shortening recovery time [1]. They can also be engaged to avoid exposing workers to the hazardous and tight spaces such as in duct cleaning and disabling a bomb. In these applications, the operator could send a small scale robot to perform the task. In addition, similar to the unmanned aerial vehicles, tele-operated robot aircrafts have been increasingly employed in military applications [2]. A robotic spacecraft is a spacecraft usually with no on-board human operator, and remotely controlled. Considering its lower cost and lower risk, many space missions prefer tele-operations than crewed operations. As we know, even provided with the most advanced equipment today, it is still too hard for human beings to perform tasks in some planetary destinations such as Venus or the vicinity of Jupiter. For even further planets such as Saturn, Uranus, and Neptune, telerobot deployment is the only possible way of exploration because of the huge distance to reach them with current crewed spaceflight technology.

Over the years, scientists and engineers in aerospace technology have made tremendous efforts to develop telerobots capable of operating and conducting tasks using tools and hardware designed for astronauts. In April 1993 for the first time in the history of space flight, a small multisensory robot, *ROTEX*, performed a number of prototype tasks on-board a spacecraft, in an operational mode namely preprogrammed remote control by the astronauts as well as remotely controlled from ground via the human operator and machine intelligence [3]. The key technologies behind the success of ROTEX were mainly multisensory gripper, local sensory feedback control, and efficacious delay-compensating 3D-graphics simulation used in the ground station [4]. German Aerospace Center has introduced in 2009 their robot, *Justin*, a wireless robot controllable through tele-presence. Justin is not only light-weighted, but owns multiple senses and can be controlled from the Earth when it works in satellite or the international space station [5]. After launching the first model of humanoid space robot *Robonant* [6], NASA Johnson Space Center has recently released the latest Robonaut version in 2011 [7]. With higher dexterity, deeper and wider range of sensing, Robonaut 2 is capable of working side-by-side with astronauts under the same environments.

Much research effort has been made during the last decade on developing neural interfaces for controlling various devices from prosthetics to telerobots. The Electromyography (EMG) is a physiological signal generated by muscle cells, and reflects the activation of neurons that control the muscle contraction. As a non-invasive means, surface EMG signals have been widely employed to detect motion information from a specific user in his/her movement intention, and thus could be utilized in the control interface for telerobots. Applications in EMG based motion recognition basically fall into three categories: controlling prosthetic limbs [8], [9], [10], rehabilitation [11], [12], and tele-robotics [13], [14]. EMG signal has been found very useful in classification of human movements [15]. Because the major driven force for human hand movements is from the extrinsic muscles in the forearm, we could estimate the manipulation force of a human hand in a specific action from the arm EMG signal [16], [17]. EMG signals have also been employed for tele-operation of robotic manipulations. Fukuda et al. proposed a human-assisting manipulator tele-operated by EMG signals and arm motions [13]. Two-dimensional myoelectrical control on a robotic arm for upper limb amputees has been achieved in [18]. An EMG-based robot arm control strategy using low-dimensional embeddings has been reported in [14]. EMG signals can also be applied in detecting muscle fatigue and signal compensation [19], [20].

Being sometimes referred to as myoelectric activity, EMG is a technology to study muscle electrical signals generated by muscle contractions. Surface EMG is a bi-dimensional electrical field on the skin surface generated by the summation of action potentials of what active motor units (MU) generates [21]. The combination of the muscle fiber action potentials from all the muscle fibers of a single MU is the motor unit action potential (MUAP). Temporal and spatial evolution of this field might be sampled by surface electrodes appropriately positioned above active muscle regions [21]. Another type of EMG records electrical impulses of a piece of muscle by inserting needles into the muscle rather than attaching electrode onto the skin surface, but this is considered invasive. The non-invasive method is more commonly employed, because it can be conducted by non-medical or clinical personnel, with low risk to the subject. In general, surface EMG signal amplitude ranges from μV to mV [22]. The amplitude, time-frequency characteristics and measurements of EMG signals depend on a few factors as follows [23]:

- timing and intensity of muscle contraction,
- distance of electrode from the active muscle area,
- attributes of overlying tissue, e.g., thickness of overlying skin and adipose tissue,
- electrode and amplifier specifications,
- quality of contact between electrode and skin.

It is well known that the variability caused by non-muscular factors that affect EMG recording could be minimized by suitably choosing relevant signal conditioning parameters and normalization methods [21]. The accuracy of measuring and representing of the EMG signal depends on the properties of the electrodes, their interaction with the skin, the amplifier design, and the conversion and subsequent storage of the EMG signal from analog to digital form (i.e., A/D conversion) [23]. The quality of the measured EMG is often described by the ratio between the measured EMG signal and unwanted noise contributions from the environment. It is desired to maximize the amplitude of the signal and to minimize the noise. Due to the small magnitude of the signal picked up at the electrode, typically a differential amplifier is employed as a first stage amplifier. Additional amplification stages may follow. Before being displayed or stored, the signal can be processed to eliminate low-frequency or high-frequency noise, or other possible artifacts [21].

As mentioned above, EMG signal is the train of MUAP reflecting the muscle response to neural stimulation. The EMG signal appears random in nature and is generally modeled as a filtered impulse process like that depicted by Equation (1) [24], where $x(n)$ is the EMG signal, $e(n)$ refers to the firing impulse, $h(r)$ represents a train of MUAP, acting as a filter,

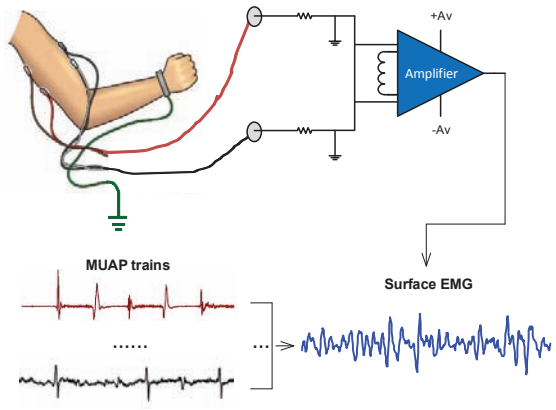

Figure 1. Surface EMG data acquisition and inclusive MUAP trains.

$w(n)$ is a zero mean addictive white Gaussian noise, and N is the number of MU firings. The impulse process stands for the neuron pulses, which is often modeled as a Poisson process [22]. Figure 1 shows the process of acquiring EMG signal and illustrates the inclusive MUAP trains as well.

$$x(n) = \sum_{r=0}^{N-1} h(r)e(n-r) + w(n). \tag{1}$$

It has been shown that surface EMG signals are highly correlated with joint stiffness and the correspondingly generated muscle tensions [25], [26]. However, when continuous movement of joints is required, highly sophisticated signal processing approaches should be applied to the segments of EMG signals, which inevitably introduce latency and increase the complexity of the scheme, particularly in real time applications. Besides, in a tele-operation scenario, e.g., in spacecraft, the long-range transmission of haptic message between the local station and remote environment would greatly suffer from time delay, which could cause severe instability in the closed-loop control system. By studying how the central nervous system stabilize unstable dynamics through learning optimal impedance in [27], we have introduced a novel human-like learning controller to interact with unknown environments [28]. In a series of pioneer works in tele-impedance control [29], [30], [31], scientists in Italy have successfully estimated and transferred human impedance to control a robot arm. Based on their impedance estimation algorithm, we propose to employ the EMG amplitudes obtained by AM-FM decomposition method, and to further combine with the force estimation technique we developed before [32] for achieving impedance and force control. In addition, for the processing of EMG signal, only high frequency band is engaged in order to avoid effects of muscle fatigue. By making use of an online impedance estimation scheme, our method would be able to tackle the challenges of instability in controlling a remote telerobot, which is especially desirable in the context of space applications. In the outlined paradigm of EMG based tele-operation system, we focus on timely capturing and transferring the human operator's muscle impedance to a telerobot. To explore human muscle impedance, we employ a new and systematic approach to extract inherent features from EMG signals. Preliminary experiment set up on a simulated robot arm is given to demonstrate our performance.

2. IMPEDANCE AND FORCE CONTROL STRATEGY

In this paper, we consider the dynamics model of a rigid telerobot manipulator, defined in the Cartesian space

$$M_r(x)\ddot{x} + C_r(x,\dot{x})\dot{x} + G_r(x) = F_x + F_r, \tag{2}$$

where $M_r(x)$ is the symmetric bounded positive definite inertia matrix; $C_r(x,\dot{x})\dot{x} \in \mathbb{R}^{\geq}$ denotes the Coriolis and Centrifugal force; $G_r(x) \in \mathbb{R}^{\geq}$ is the gravitational force, which can be ignored when the robot operates in remote space far from the earth; F_x is the vector of equivalent control input in Cartesian space, and we can easily calculate the joint torque input by using $\tau = J^T F_x$ where J is the geometric Jacobian matrix; and $F_r \in \mathbb{R}^{\geq}$ is the interactive force applied on the the end-effector.

The motion reference trajectory x^* is set by human operator remotely, usually by using a joystick or motion tracking device. To make the robot manipulator track the reference trajectory x^*, the telerobot employs the following control law [28]:

$$F_x = -F - Ke - D\dot{e} - L\varepsilon + F_r, \tag{3}$$

where

$$e \equiv x - x^*, \quad \dot{e} \equiv \dot{x} - \dot{x}^*,$$

are respectively *position error* and *velocity error* relative to the task reference trajectory, and

$$\varepsilon \equiv \dot{e} + \kappa e, \quad \kappa > 0,$$

is the *filtered error* commonly used in robot control. In the controller (3), $-F$ is the *feedforward* force, which is usually used to compensate for constant or periodic external force, and $-Ke - D\dot{e}$ is the *feedback* force used to compensate for unpredictable external force. The stiffness K and damping D will be learned through interaction with the environment. The term $-L\varepsilon$ corresponds to the desired *stability margin*, where L is a symmetric positive definite matrix that help to ensure stable compliant motion. Inhuman arm, this minimal feedback is produced by passive mechanical properties of muscles without contraction and reflexes [33]. In addition, one could employ the following F_r

$$F_r(t) \equiv M\ddot{x}^* + C\dot{x}^* + G. \tag{4}$$

to compensate for robot/arm dynamics and bounded noise.

In the framework set up in this paper, the feedforward F will be obtained by estimation of operator's force from EMG signals, the stiffness K will also be estimated from human operator's muscle EMG, and for simplicity, we set damping as below:

$$D = 2\sqrt{K}, \tag{5}$$

with square root $\sqrt{(\cdot)}$ is defined component-wise.

3. SIGNAL PROCESSING OF EMG

In this section, we first observe the primary amplitude-frequency modulation components in EMG signals, and then introduce the EMG feature set applicable for movement detection and relevant pattern recognition tasks in robotics.

Signal decomposition and processing

A narrow-band signal, whose bandwidth is sufficiently small, can be viewed as a monocomponent amplitude and frequency modulating (AM-FM) signal. Among the frequencies spanning over the signal spectrum, there is one frequency bin assuming a majority of the signal energy. The two determining parameters in an AM-FM signal are *amplitude* and *phase*. A *monocomponent* AM-FM signal is described by Equation (6) [34],

$$x(n) = A(n)cos\big[\Theta(n)\big], \tag{6}$$

where $A(n)$ denotes the instantaneous amplitude of the monocomponent signal and $\Theta(n)$ denotes its instantaneous phase.

EMG signals are the superposition of activities of multiple motor units. It is necessary to decompose the EMG signals to reveal the mechanisms pertaining to muscle and nerve control. Various techniques have been devised with regards to EMG decomposition. The kth MUAP sequence $s_k(n)$ in an EMG signal as shown in Figure 1 could be formulated as an AM-FM term by Equation (7):

$$s_k(n) = A_k(n)cos\big[\Theta_k(n)\big], \tag{7}$$

with the MUAP train being characterized by two sequences:

- $A_k(n)$ – Amplitude;
- $\Theta_k(n)$ – Phase.

EMG signal decomposition has been done by wavelet spectrum matching in work by Fang et al. [35], where they measured waveform similarity of single motor unit potentials from wavelet domain. Plevin et al. have proposed to use non-linear least mean square optimization of higher-order cumulants [36]. Teagers proposed to employ a *multicomponent* AM-FM model in exploring amplitude-frequency modulation patterns in speech resonances [37]. Likewise, considering the multiple characteristic bands of EMG, we can also interpret it as a multicomponent AM-FM signal. An EMG signal can thus be written as a linear combination of amplitude and frequency modulated components which we call the primary components,

$$\begin{aligned} s(n) &= \sum_{k=1}^{K} A_k(n)cos[\Theta_k(n)] + \eta(n) \qquad (8)\\ &= \sum_{k=1}^{K} A_k(n)cos\left\{\left[\Omega_c(k)n + \sum_{r=1}^{n} q_k(r)\right]\right\} + \eta(n), \end{aligned}$$

where $A_k(n)$ denotes the instantaneous amplitude of the kth primary component and $\Theta_k(n)$ denotes its instantaneous phase. With the backward difference between $\Theta_k(n)$ and $\Theta_k(n-1)$, the instantaneous frequency sequence is defined as $\Omega_k(n) = \Omega_c(k) + q_k(n) = \frac{2\pi}{f_s} f_c(k) + q_k(n)$, where f_s is the sampling frequency, and $q_k(n)$ is the frequency modulation component. Note $\eta(n)$ takes into account additive noise and errors of modeling, especially those errors due to finite summation. The dominant MUAP trains in an EMG signal are therefore captured by the primary AM-FM components in the corresponding frequency bands. Depending on applications, the number of primary components required for processing may vary. For the stiffness and force estimation purpose in this study, the necessary components are identified as the existing constituent muscle electrical waves.

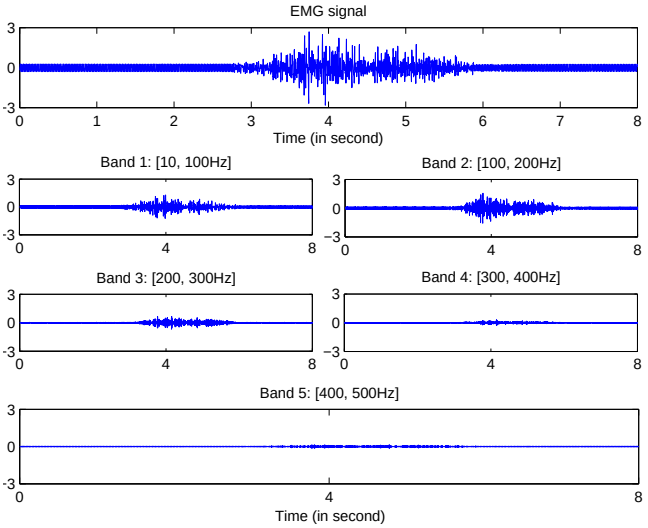

Figure 2. A 8-second long EMG signal and its decomposed waves in 5 frequency bands (Band 1: [10, 100Hz], Band 2: [100, 200Hz], Band 3: [200, 300Hz], Band 4: [300, 400Hz], and Band 5: [400, 500Hz]).

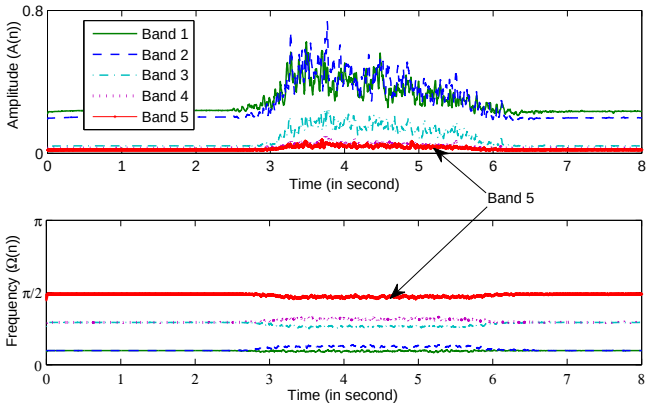

Figure 3. The instantaneous amplitude estimate $A(n)$ and frequency estimate $\Omega(n)$ in the decomposed EMG waves.

Figure 2 gives an example of a 8-second long EMG signal and the present primary components detected through band-pass filtering. In Figure 3, instantaneous amplitudes and frequencies of these subbands have been shown. As an example, estimates from Band 5 of the EMG signal have been denoted in red color. It is obvious that a primary component dominates each subband, and this principal value differs from one subband to another. This could be an efficient method to detect and identify the EMG amplitude element of interest.

Feature Extraction

An important step in EMG signal processing and relevant classification tasks is feature extraction, which reveals the underlying patterns. We employ the multi-band AM-FM model on the EMG signal to extract two feature vectors on a segment-by-segment basis: the averaged instantaneous envelope (AIE) and the averaged instantaneous frequency (AIF). The process of computing the AIE and AIF features is summarized as follows:

1. *Preprocessing*: The raw EMG signal is digitally sampled at 2K Hz using NI USB 6210 device, and band-pass filtered from 10 to 500 Hz using a digital fourth-order Butterworth filter. It is further notch filtered at 50 Hz to remove line-frequency noise.
2. *Signal segmentation*: The signal in each channel is segmented into 100 *ms* segments with no overlap for minimum delay in real-time control system [38].
3. *Signal decomposition*: Each segment is divided into 5 subbands: 10-100 Hz, 100-200 Hz, 200-300 Hz, 300-400 Hz, and 400-500 Hz through a bank of 48th ordered finite impulse response (FIR) filters, where a 48-point Hanning window is applied before the filtering process.
4. *Multi-band demodulation*: Teager's energy separation algorithm [34] is employed to obtain the instantaneous envelope (IE) sequence $|A(n)|$ and the instantaneous angular frequency (IF) $\Omega(n)$ one segment after another for each subband signal.
5. *Sequence smoothing*: A 21-point median filter is applied to remove the abrupt impulses in the segments of IE and IF sequences, where the order 21 is empirically determined.
6. *Spatio-temporal averaging*: This process is conducted on each subband segment by following a two-step calculation:
- *Temporal averaging*: The averaging operation is undertaken on the smoothed IE and IF sequences first to remove the fluctuations over time.
- *Spatial averaging*: These temporal IE, IF mean values are then averaged across different channels to compensate for possible channel variability.

The commonly used features to characterize an EMG signal include time-domain parameters mean absolute value (MAV), waveform length (WL), and frequency-related auto-regression coefficients (AR). There are studies on comparing these parameters among other features for EMG [39], [40]. However, the signal decomposition by AM-FM demodulation has provided us a systematic way to investigate the underlying properties existing in an EMG signal. The short-term parameter sets AIE and AIF generated from the characteristic bands of EMG signals are found capturing the dominant amplitude and frequency components in the concerned temporal span and spatial range of these bands. The dimension of AIE and AIF feature vectors depends on the number of subbands that are included, which is largely related with the applications. Considering the rich signal characteristics contained in the AIE and AIF parameters, and their inherent denoising capability, these two sets of features have proven their efficacy in discriminating Electroencephalogram (EEG) samples from healthy subjects and epilepsy patients [41]. It is believed that these features can also provide distinct perspective in EMG signal processing.

4. STIFFNESS AND FORCE ESTIMATION

This section describes the theory and process of estimating the endpoint stiffness and force from muscle EMG signal.

Stiffness estimation

It is well known that human muscles and tendons act as a spring-damper system during movement, and they together play a critical role for stabilization and energy storage. Muscle stiffness in the stretch reflex is also noted largely proportional to the muscle tension [42]. Human beings can change the size of endpoint stiffness ellipse [22], [27], whose central nervous system is able to regulate the stiffness of the joint in its equilibrium angle independent of the generated torque/force through the co-activation of antagonistic muscle pairs. Muscle and peripheral reflex loops possess spring-like properties that pull joints back to equilibrium positions by generating restoring forces against external perturbations. This viscoelasticity can be regarded as the peripheral feedback control gain, which is adjustable by regulating muscle co-contraction levels and reflex gains [25]. Considering this, Ajoudani et al. suggested to accomplish tele-operation tasks by adjusting co-activations and corresponding endpoint stiffness profile, and by using indexes of co-contractions for the sake of endpoint stiffness estimation [29], [30], [31].

In an attempt to estimate force from surface EMG signal, Potvin et al. have found that EMG amplitude in the low frequency region can increase with force changes being absent. During fatigue, it happens that there are increases in the low frequency EMG power also with force unchanged. They therefore thought it is not optimal to use the whole band of raw EMG signal (which roughly ranges 20-500 Hz), instead, they discarded up to 99% of the signal power before estimating muscle force and ended up with an improved result [43]. In a similar manner, in order to obtain the stiffness from EMG measurements, we consider first decomposing the EMG signal along the frequency axis and involving only the highest frequency band in the estimation process, which is 400-500 Hz (Band 5) in our study.

Basmajian and De Luca have found that rectified surface EMG signals are proportional to isometric muscle tension and highly correlated with static and dynamic stiffness [22]. The length and velocity dependency of the generated muscle tensions actually demonstrate nonlinear behaviours. Ajoudani et al. in their recent works have assumed a linear mapping between muscle tensions and generated surface EMGs with constant moment arms around the task space, which is in a way close to isometric conditions [29], [30], [31]. Grounded on the work of Osu et al. on monitoring elastic behavior of human arm endpoint using muscle co-contraction index, the research in [29], [30], [31] worked out the expressions for the endpoint torque. Based on their algorithm, we replace the EMG amplitude from the entire signal with those from the highest band of the decomposed EMG signal, and end up with modified solutions shown by equation array in Equation (9):

$$\begin{aligned} f^h_{ex}(n) &= \sum_{i=1}^{p} \alpha_i A^i_{ago}(n) - \sum_{j=1}^{p} \beta_j A^j_{anta}(n), \\ f^h_{ey}(n) &= \sum_{i=1}^{p} \alpha'_i A^i_{ago}(n) - \sum_{j=1}^{p} \beta'_j A^j_{anta}(n), \\ f^h_{ez}(n) &= \sum_{i=1}^{p} \alpha''_i A^i_{ago}(n) - \sum_{j=1}^{p} \beta''_j A^j_{anta}(n), \end{aligned} \tag{9}$$

where $f^h_{ex}(n)$, $f^h_{ey}(n)$ and $f^h_{ez}(n)$ denote the endpoint forces of human arm in Cartesian coordinates x, y and z at time point n, respectively. To distinguish from that in [29], [30], [31], a superscript h is attached to implicate the high frequency EMG signal engaged in our calculation. $A^i_{ago}(n)$ and $A^j_{anta}(n)$ are amplitude values of pre-processed EMG signals measured at the ith agonist muscle and the jth antagonist muscle in the frequency band 400-500 Hz, respectively. Suppose there are p pairs of muscles involved, parameter set $\boldsymbol{\alpha} = [\alpha_1, \ldots, \alpha_p]$, $\boldsymbol{\beta} = [\beta_1, \ldots, \beta_p]$, $\boldsymbol{\alpha}' = [\alpha'_1, \ldots, \alpha'_p]$, $\boldsymbol{\beta}' = [\beta'_1, \ldots, \beta'_p]$, $\boldsymbol{\alpha}'' = [\alpha''_1, \ldots, \alpha''_p]$, $\boldsymbol{\beta}'' = [\beta''_1, \ldots, \beta''_p]$ each contains p coefficients to be estimated, respectively. Like

in [29], [30], [31], the above equations were solved offline to obtain the parameter vector $[\boldsymbol{\alpha}, \boldsymbol{\beta}, \boldsymbol{\alpha}', \boldsymbol{\beta}', \boldsymbol{\alpha}'', \boldsymbol{\beta}'']$. If the interaction forces f_{ex}^h, f_{ey}^h and f_{ez}^h between the operator and the joystick is measurable, we propose in this work to solve these parameters by iterative least squares (LS) approach to achieve online estimation. As a commonly used way to obtain a model from a set of data, LS is usually carried out on the following linear regression model:

$$y(n+1) = \boldsymbol{\theta}^\tau \boldsymbol{\phi}_n + w(n+1). \tag{10}$$

Let us rewrite each equation in Equation (9) into the form of Equation (10). First, let sequence y be f_{ex}^h, which represents observation/system output. $\boldsymbol{\phi}_n$ is the regressor at time instant n, which equals to $[A_{ago}(n), \ldots, A_{ago}(n-p+1), A_{anta}(n), \ldots, A_{anta}(n-p+1)]$, and w stands for the noise processes/sequences. We use vector $\boldsymbol{\theta}$ to denote the unknown parameter vector $[\boldsymbol{\alpha}, \boldsymbol{\beta}]$, and it will be estimated by minimizing the following criteria:

$$J_n(\boldsymbol{\theta}) = \frac{1}{2}\sum_{k=0}^{n-1}(y(k+1) - \boldsymbol{\theta}^\tau \boldsymbol{\phi}_k)^2. \tag{11}$$

Denote the estimated value of $\boldsymbol{\theta}$ at the nth sampling point as $\boldsymbol{\theta}_n$, the next step estimation $\boldsymbol{\theta}_{n+1}$ is calculated by the recursive LS algorithm as follows

$$\boldsymbol{\theta}_{n+1} = \boldsymbol{\theta}_n + \boldsymbol{L}_n(y_{n+1} - \boldsymbol{\theta}_n^\tau \boldsymbol{\phi}_n), \tag{12}$$

where $\boldsymbol{P}_{n+1} = \boldsymbol{P}_n - \frac{\boldsymbol{P}_n \boldsymbol{\phi}_n \boldsymbol{\phi}_n^\tau \boldsymbol{P}_n}{1+\boldsymbol{\phi}_n^\tau \boldsymbol{P}_n \boldsymbol{\phi}_n}$, and $\boldsymbol{L}_n = \frac{\boldsymbol{P}_n \boldsymbol{\phi}_n}{1+\boldsymbol{\phi}_n^\tau \boldsymbol{P}_n \boldsymbol{\phi}_n}$. In the similar manner, we estimate parameter vectors $[\boldsymbol{\alpha}', \boldsymbol{\beta}']$ and $[\boldsymbol{\alpha}'', \boldsymbol{\beta}'']$.

Note this iterative approach provides estimated $\boldsymbol{\theta}$ values along the time line. The endpoint force and stiffness estimation can also be calculated in an online manner, where real-time control can be achieved. Based on the proportional relationship between muscle stiffness and torque, the endpoint stiffness of human arm under Cartesian coordinates can be obtained as expressed by Equation (13) [25].

$$\begin{aligned} K_{xx}(n) &= \sum_{i=1}^{p} |\alpha_i| A_{ago}^i(n) + \sum_{j=1}^{p} |\beta_j| A_{anta}^j(n), \\ K_{yy}(n) &= \sum_{i=1}^{p} |\alpha_i'| A_{ago}^i(n) + \sum_{j=1}^{p} |\beta_j'| A_{anta}^j(n), \\ K_{zz}(n) &= \sum_{i=1}^{p} |\alpha_i''| A_{ago}^i(n) + \sum_{j=1}^{p} |\beta_j''| A_{anta}^j(n). \end{aligned} \tag{13}$$

Then, $K = \text{diag}(K_{xx}, K_{yy}, K_{zz})$ will be substituted in the telerobot controller defined in Equation (3).

Force estimation

The feedforward force F in the telerobot controller defined by Equation (3) can be obtained by extension of the joint torque estimation we proposed in [32], where the combined techniques of Kalman filter and nonlinear normalization have been successfully engaged in estimating human joint forces. For this propose, the EMG signal amplitude from the frequency band 400-500 Hz is employed to discard most of the power energy in the low frequency range typically caused by muscle fatigue, tissue filtering properties and the differential amplification process, and is further nonlinearly normalized as described below. It is reported that in larger muscles where the firing rate has a lower dynamic range, the relationship between force and the amplitude of EMG signal can be described by the nonlinear Equation (14) [44],

$$A_N^h = 100\frac{e^{(-A_L^h \xi)} - 1}{e^{-100\xi} - 1}, \tag{14}$$

where A_L^h is obtained by linearly normalizing the extracted amplitude A^h to 100% of the maximum amplitude. Then, by passing A_N^h through a Kalman filter and calculating it from a pair of agonist and antagonist muscles with a certain joint, we can get a torque estimate for it. The force estimated in this section can be easily transformed to end-effector force in Cartesian space using generalized inverse of Jacobian matrix of the human operator arm.

5. WORKING FRAMEWORK

Stable manipulation of the proposed tele-robotic system in aerospace application domains is conducted through measuring muscular attributes from human muscle and transferring them to the remote robot in real time. In most skeletal muscles, the EMG activity precedes the motion of the actuated limb at the range of 50-100 *ms* [45]. This advantage of EMG can be effectively taken in our proposed signal processor. The signal processing front-end employed in this paper distinguishes it from most of current works in that it can provide comprehensive yet simple EMG representation, from which efficient muscular message can be generated. By combining the algorithm introduced in [30] with the AM-FM decomposition technique, we propose a method to estimate human impedance from the acquired EMG signals. In addition, force estimation from human operator is also considered in this work. As a preliminary attempt towards EMG enhanced impedance and force control system for telerobots engaged in aerospace tasks, the herein provided framework is comprehensive yet still extendable by potential users.

Figure 4 gives an overall illustration of the EMG enhanced impedance and force control based tele-operation system in a typical aerospace operation scenario. This depicted paradigm mainly contains three modules: EMG data acquisition, signal processing & feature extraction, and robotic control. The input data are continuously recorded surface EMG measurements from the local operator, which could be any personnel in charge of the operation task. These time-varying sequences are then processed by a series of signal processing steps, producing respective myoelectrical profiles of the concerned muscle, which are named feature vectors in pattern recognition terminology. Through implementing these sequentially connected procedures, which include temporal segmentation, spectral decomposition, and multi-band demodulation on the EMG signal, its instantaneous amplitude and frequency sequences are picked out, respectively. The most dominant amplitude component present in the signal is then extracted to provide online endpoint stiffness and force estimates, where they are immediately transferred from local operator to the remote robot to ensure minimum delay. A telerobot controller dedicated to dealing with unknown interactions is applied. Furthermore, the EMG feature vectors extracted in the second module can be employed to perform other classification tasks, such as motion recognition and intention detection. This infrastructure built for tele-operating robots in aerospace applications provides necessary signal processing steps to

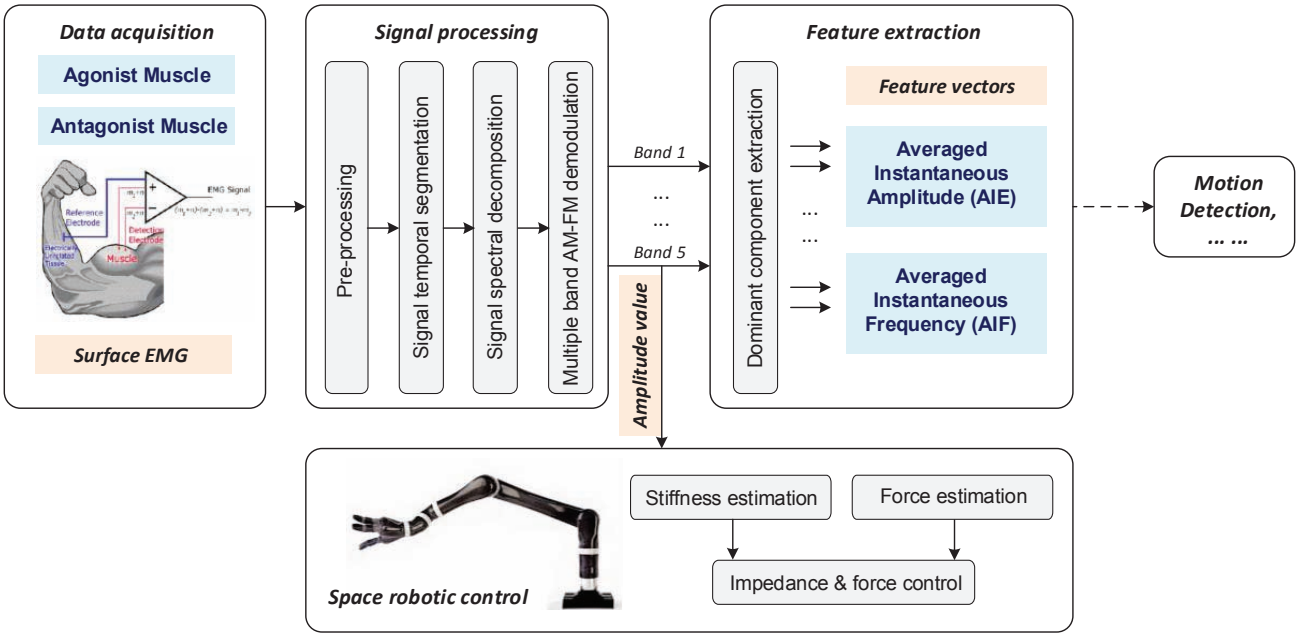

Figure 4. A paradigm of EMG enhanced impedance and force control for telerobot operation in space (The Kinova JACO robot arm [46] is taken for illustration purpose).

handle various physiological signals beyond EMG, which could be EEG for instance. In consequence, the integrated and portable structure of the proposed framework make it applicable to a range of other domains not included in the scale of this study.

6. IMPEDANCE CONTROL SIMULATION

To demonstrate the impedance control performance of our EMG enhanced impedance and force control method, a two-joint arm is simulated and animated using Matlab Robotics Toolbox [47] in Simulink. In this preliminary study, we omit force estimation which was done in our previous work [32] for simplicity. During the test, we consider simple posture control only, i.e., the motion reference trajectory is reduced to be at the initial position. The right wrist of the human operator, which is in charge of the simulated robot manipulator's motion, is supposed to hold still through the whole process. The first joint (elbow) of the simulated robot arm is fixed (i.e., motionless) while only the second joint (wrist flexion/extension joint) is controlled. At the beginning of the experiment, the simulated robot arm rests in the initial position of 0 *rad*, and then some randomly generated disturbances are exerted on its wrist. Due to the disturbance forces which are random in magnitude and direction, the forearm tends to shake around initial position for some moment. This will be observed by the human operator via vision feedback. Then, the human operator will subsequently clench fist to stiffen wrist joint, in order to increase wrist joint impedance. The increased impedance will be reflected by the increasing of EMG magnitude. During this process, for simplicity only two-channeled EMG data are acquired to reflect the human operator's wrist motion, e.g., extensor carpi radialis and flexor carpi ulnaris. Note that in this simple illustration, we have omitted force control, and only consider motion in a single joint. Because of the small range of motion angle, motion only occurs in x-axis. The parameter vector $[\alpha, \beta]$ is estimated offline when the wrist is sustaining a set of constant forces against a spring scale in isometric condition. Then, with the online EMG processing module in our proposed framework, the stiffness K and damping rate D are obtained as described in Section 4 every 100 *ms* and are immediately transferred to the simulated manipulator for online impedance control. The experimental setup is shown in Figure 5.

To illustrate the simulation performance clearly, Figure 6 shows the stiffness estimate K and damping rate estimate D of the slave manipulator obtained during the simulation time interval. An evident difference in $[K, D]$ values is identified to divide their variations into two stages. In the first stage, both K and D are steady and relatively small at relaxed condition. While with the fisting motion, $[K, D]$ have been multiplied manifold. On the other hand, Figure 7 records the shift angles of the simulated robot manipulator in due course. It is noted that the shaking amplitude is almost reduced from up to 0.25 *rad* to less than 0.04 *rad*, which means the manipulator has consequently compensated for the high frequency disturbances by taking the impedance transferred from the human operator. The consistent observations from Figures 6 and 7 fully support our approach of using human muscle EMG for real-time telerobot impedance control.

7. CONCLUSION AND FUTURE WORK

In order to better transfer human operator's control strategies to a telerobot to improve control performance, an EMG enhanced impedance and force control framework has been proposed in this paper. Transferring human operator's arm impedance in real time to a tele-operated robot will not only

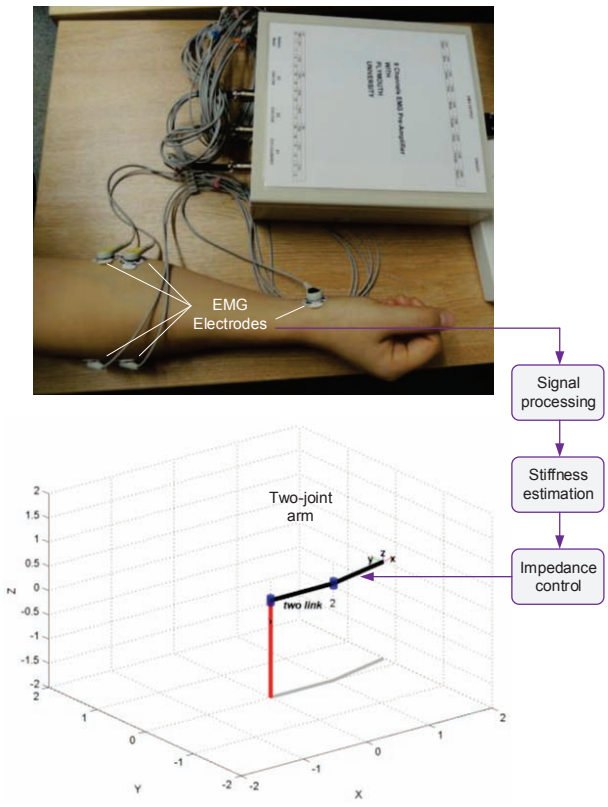

Figure 5. Impedance control simulation set up on a two-joint arm.

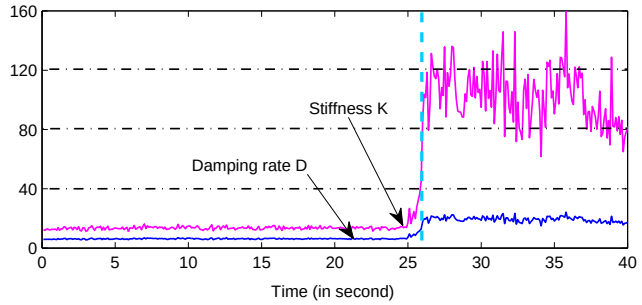

Figure 6. Estimated stiffness K and damping rate D of the slave manipulator (second joint) over time.

help to reduce possible instability caused by communication time delay, but also enhance the control performance by enabling the robot to fully capture operator's control skills. Due to the wide use of EMG in prosthetic limb control, rehabilitation, and tele-robotics, EMG signals have been taken as an essential carrier of intrinsic muscular activity. We therefore focus on extracting and transferring impedance and force information from human muscle EMGs to achieve impedance and force control of a remote robot under the tele-operation protocol, especially in the context of space robot applications. In our proposed framework, we provide a compact yet comprehensive form for EMG feature extraction by means of efficient signal processing, together with an

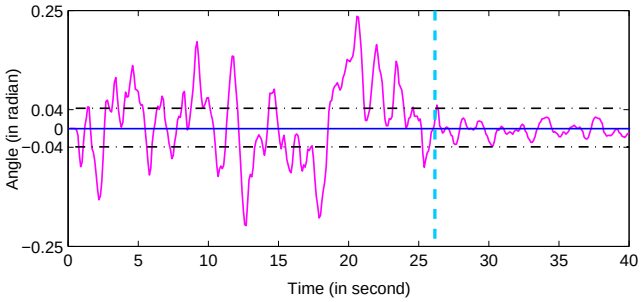

Figure 7. Angle shifting of the slave manipulator from original position (zero angle) measured in radian.

online estimation strategy for stiffness and force. In a preliminary simulated experiment, our framework of capturing and transferring muscle impedance from EMG to the simulated robot arm has been tested, showing desirable performance. It is expected that the herein introduced framework will provide new perspective in promoting tele-robotics research. Complete experimental studies on physical robot arm is planned to be carried out in our future work, so as to test and validate the proposed methods presented in this paper.

ACKNOWLEDGMENTS

The authors thank Dr. Hai Li who built the amplifier for EMG data collection, Mr. Stuart Manning who provided raw EMG data for analysis, and Mr. Peidong Liang who assisted in setting up the simulation platform and helped to collect EMG signals for simulation. The work was supported in part by grants from the Research Grants Council of the Hong Kong Special Administrative Region, China (Project No. CUHK 415113 of General Research Fund and Project No. N_CUHK405/11 of the NSFC/RGC Joint Research Scheme), and by the Royal Society International Exchange Grant (IE130681) and Royal Society Research Grant (RG130244).

REFERENCES

[1] G. Cadiere, J. Himpens, and O. Germay, "Feasibility of robotic laparoscopic surgery: 146 cases," *World Journal of Surgery*, vol. 25, no. 11, pp. 1467–1477, 2001.

[2] T. Fong and C. Thorpe, "Vehicle teleoperation interfaces," *Autonomous robots*, vol. 11, no. 1, pp. 9–18, 2001.

[3] J. D. J. H. G. Hirzinger, B. Brunner, "Sensor-based space robotics-ROTEX and its telerobotic features," *IEEE Tran. Robotics and Automation*, vol. 9, no. 5, pp. 649–663, 1993.

[4] G. Hirzinger, B. Brunner, J. Dietrich, and J. Heindl, "ROTEX: the first remotely controlled robot in space," in *Proc. Robotics and Automation*, 1994, pp. 2604–2611.

[5] http://www.firstdigest.com/2009/03/cebit-2009-justin-the-robot-tea-preparer/.

[6] R. Ambrose, H. Aldridge, R. Askew, R. Burridge, W. Bluethmann, M. Diftler, C. Lovchik, D. Magruder, and F. Rehnmark, "Robonaut: NASA's space humanoid," *IEEE Intelligent Systems*, pp. 57–62, 2000.

[7] M. Diftler, J. Mehling, M. Abdallah, N. Radford, L. Bridgwater, A. Sanders, R. Askew, D. Linn, J. Yamokoski, F. Permenter, B. Hargrave, R. Platt, R. Savely, and R. Ambrose, "Robonaut 2: the first humanoid robot in space," in *Proc. ICRA*, 2011, pp. 2178–2183.

[8] F. Tenore, A. Ramos, A. Fahmy, S. Acharya, and R. Etienne-Cummings, "Towards the control of individual fingers of a prosthetic hand using surface EMG signals," in *Proc. EMBC*, 2007, pp. 6145–6148.

[9] C. Castellini and P. van der Smagt, "Surface EMG in advanced hand prosthetics," *Biol. Cybernet.*, vol. 100, no. 1, pp. 35–47, 2009.

[10] D. Zhang, X. Chen, S. Li, P. Hu, and X. Zhu, "EMG controlled multi-functional prosthetic hand: Preliminary clinical study and experimental demonstration," in *Proc. ICRA*, 2011, pp. 4670–4675.

[11] P. Langhorne, F. Coupar, and A. Pollock, "Motor recovery after stroke: A systematic review," *Lancet Neurol.*, vol. 8, no. 8, pp. 741–754, 2009.

[12] N. Ho, K. Tong, X. Hu, K. Fung, X. Wei, W. Rong, and E. Susanto, "An EMG-driven exoskeleton hand robotic training device on chronic stroke subjects: Task training system for stroke rehabilitation," in *Proc. ICRR*, 2011, pp. 1–5.

[13] O. Fukuda, T. Tsuji, M. Kaneko, and A. Otsuka, "A human assisting manipulator teleoperated by EMG signals and arm motions," *IEEE Trans. Robotics and Automation*, vol. 19, pp. 210–222, 2003.

[14] P. Artemiadis and K. Kyriakopoulos, "EMG-based control of a robot arm using low-dimensional embeddings," *IEEE Trans. Robotics*, vol. 26, pp. 393–398, 2010.

[15] Z. Ju and H. Liu, "Human hand motion analysis with multisensory information," *IEEE/ASME Trans. Mechatronics*, vol. PP, no. 99, pp. 1–11, Feb. 2013.

[16] T. Saponas, D. Tan, D. Morris, R. Balakrishnan, J. Turner, and J. Landay, "Enabling always-available input with muscle-computer interfaces," in *Proc. ACM Annual Symposium on User Interface and Software Technology*, 2009, pp. 167–176.

[17] X. Tang, Y. Liu, C. Lv, and D. Sun, "Hand motion classification using a multi-channel surface electromyography sensor," *Sensors*, vol. 12, no. 2, pp. 1130–1147, 2012.

[18] N. Celani, C. Soria, E. Orosco, F. di Sciascio, and M. Valentinuzzi, "Two-dimensional myoelectric control of a robotic arm for upper limb amputees," *J. Phys. Conf. Ser.*, vol. 90, 2007.

[19] P. Artemiadis and K. Kyriakopoulos, "An EMG-based robot control scheme robust to time-varying EMG signal features," *IEEE Trans. Information Technology in Biomedicine*, vol. 14, pp. 582–588, 2010.

[20] ——, "A switching regime model for the EMG-based control of a robot arm," *IEEE Trans. Systems, Man, and Cybernetics, Part B*, vol. 41, pp. 53–63, 2011.

[21] A. Botter, M. Gazzoni, and R. Merletti, *Surface Electromyogram detection*, ser. IEEE Press Series in Biomedicl Engineering. Piscataway, NJ: Wiley, 2013, ch. 6, pp. 113–137.

[22] J. Basmajian and C. de Luca, *Muscles alive: the functions revealed by Electromyography*. Baltimore, MD: Williams and Wilkins, 1985.

[23] B. Gerdle, S. Karlsson, S. Day, and M. Djupsjöbacka, *Acquisition, processing and analysis of the surface Electromyogram*. Berlin: Springer Verlag, 1999, ch. 26, pp. 705–755.

[24] M. Reaz, M. Hussain, and F. Mohd-Yasin, "Techniques of EMG signal analysis: detection, processing, classification and applications," *Biological Procedures*, vol. 8, no. 1, pp. 11–35, 2006.

[25] R. Osu, D. Franklin, H. Kato, H. Gomi, K. Domen, T. Yoshioka, and M. kawato, "Short- and long-term changes in joint co-contraction associated with motor learning as revealed from surface EMG," *J. Neurophysiol.*, vol. 88, pp. 991–1004, 2002.

[26] P. Artemiadis and K. Kyriakopoulos, "EMG-based position and force control of a robot arm: Application to teleoperation and orthosis," in *Proc. IEEE/ASME Avdanced Intelligent Mechatronics*, 2007, pp. 1–6.

[27] E. Burdet, R. Osu, D. W. Franklin, T. E. Milner, and M. Kawato, "The central nervous system stabilizes unstable dynamics by learning optimal impedance," *Nature*, vol. 414, no. 6862, pp. 446–449, 2001.

[28] C. Yang, G. Ganesh, A. Albu-Schaeffer, and E.Burdet, "Human like adaptation of force and impedance in stable and unstable tasks," *IEEE Transactions on Robotics*, vol. 27, no. 5, pp. 918–930, 2011. [Online]. Available: http://dx.doi.org/10.1109/TRO.2011.2158251

[29] A. Ajoudani, N. G. Tsagarakis, and A. Bicchi, "Tele-impedance: Preliminary results on measuring and replicating human arm impedance in tele operated robots," in *Robotics and Biomimetics (ROBIO), 2011 IEEE International Conference on*. IEEE, 2011, pp. 216–222.

[30] A. Ajoudani, N. Tsagarakis, and A. Bicchi, "Tele-impedance: Teleoperation with impedance regulation using a body–machine interface," *The International Journal of Robotics Research*, vol. 31, no. 13, pp. 1642–1656, 2012.

[31] A. Ajoudani, N. G. Tsagarakis, and A. Bicchi, "Tele-impedance: Towards transferring human impedance regulation skills to robots," in *Robotics and Automation (ICRA), 2012 IEEE International Conference on*. IEEE, 2012, pp. 382–388.

[32] Z. Li, B. Wang, F. Sun, C. Yang, W. Zhang, and Q. Xie, "semg-based joint force controls for an upper-limb power-assist exoskeleton robot," *IEEE Journal of Biomedical and Health Informatics*, 2014 (in press).

[33] E. J. Perreault, R. F. Kirsch, and P. Crago, "Multijoint dynamics and postural stability of the human arm," *Experimental Brain Research*, vol. 157, no. 4, pp. 507–517, 2004.

[34] P. Maragos, J. Kaiser, and T. Quatieri, "Energy separation in signal modulations with application to speech analysis," *IEEE Trans. Signal Process.*, vol. 41, no. 10, pp. 3024–3051, Oct. 1993.

[35] J. Fang, G. Agarwal, and B. Shahani, "Decomposition of EMG signals by wavelet spectrum matching," in *Proc. EMBC*, 1997, pp. 1253–1256.

[36] E. Plevin and D. Zazula, "Decomposition of surface EMG signals using non-linear LMS optimization of higher-order cumulants," in *Proc. IEEE Symposium on Computer-based Medical System*, 2002, pp. 149–154.

[37] H. Teager, "Some observations on oral air flow during phonation," *IEEE Trans. Acoust. Speech*, vol. 28, no. 5, pp. 599–601, Oct. 1980.

[38] B. Hudgins, P. Parker, and R. Scott, "A new strategy for multifunction myoelectric control," *IEEE Trans. Biomed. Engineering*, vol. 40, no. 1, pp. 82–94, 1993.

[39] D. Tkach, H. Huang, and T. Kuiken, "Study of stability of time-domain features for electromyographic pattern recognition," *Journal of NeuroEngineering and Rehabilitation*, vol. 7, no. 21, pp. 1–13, 2010.

[40] D. Farina and R. Merletti, "Comparison of algorithms for estimation of EMG variables during voluntary isometric contractions," *J. Electromyogr. Kinesiol.*, vol. 10, pp. 337–349, 2000.

[41] N. Wang and M. Lyu, "Exploration of instantaneous amplitude and frequency features for epileptic seizure prediction," in *Proc. BIBE*, 2012, pp. 292–297.

[42] Y. Fukuoka, H. Kimura, and A. Cohen, "Adaptive dynamic walking of a quadruped robot on irregular terrain based on biological concepts," *The International Journal of Robotics Research*, vol. 22, pp. 187–202, 2003.

[43] J. Potvin and S. Brown, "Less is more: high pass filtering, to remove up to 99% of the surface EMG signal power, improves EMG-based biceps brachii muscle force estimates," *Journal of Electromyography and Kinesiology*, vol. 14, pp. 389–399, 2003.

[44] J. Potvin, R. Norman, and S. McGill, "Mechanically corrected EMG for the continuous estimation of erector spine muscle loading during repetitive lifting," *Eur. J. Appl. Physiol.*, vol. 74, p. 119C132, 1996.

[45] P. Artemiadis, "EMG-based robot control interfaces: Past, present and future," *Advances in Robotics & Automation*, vol. 1, no. 2, p. 1:e107, 2012.

[46] http://kinovarobotics.com/.

[47] P. Corke, *Robotics, vision and control: Fundamental algorithms in MATLAB®*, ser. Springer Tracts in Advanced Robotics, B. Siciliano, O. Khatib, and F. Groen, Eds. Berlin Heidelberg: Springer-Verlag, 2011, vol. 73.

BIOGRAPHY

Ning Wang *received the B.Eng. degree in measurement and control technologies and devices from the College of Automation, Northwestern Polytechnical University, Xi'an, China, in 2005, the M.Phil. and Ph.D degree in electronic engineering from the Department of Electronic Engineering, Chinese University of Hong Kong, Hong Kong, China, in 2007 and 2011, respectively. She is currently working as Post-doc fellow at the Department of Computer Science & Engineering, Chinese University of Hong Kong. Her research interests lie in signal processing and nonlinear modeling, robust speaker recognition, biomedical engineering, and intelligent data analysis.*

Chenguang Yang *obtained his B.Eng degree in measurement and control from Northwestern Polytechnical University, China, 2005, and the Ph.D degree in control engineering from National University of Singapore, 2010. He was with the Imperial College London as a Research Associate working on human robot interaction from Oct 2009 to Dec 2010. He has been with Plymouth University as a Lecturer in Robotics since Dec 2010. His current research interests include robotics, control, and human-robot interaction.*

Michael Rung-Tsong Lyu *received the B.S. Degree in Electrical Engineering from National Taiwan University, Taipei, Taiwan, China, in 1981; the M.S. Degree in Computer Engineering from University of California, Santa Barbara, in 1985; and the Ph.D. Degree in Computer Science from University of California, Los Angeles, in 1988. He was with the Jet Propulsion Laboratory as a Technical Staff Member from 1988 to 1990. From 1990 to 1992, he was with the Department of Electrical and Computer Engineering, The University of Iowa, Iowa City, as an Assistant Professor. From 1992 to 1995, he was a Member of the Technical Staff in the applied research area of Bell Communications Research (Bellcore), Morristown, New Jersey. From 1995 to 1997, he was a Research Member of the Technical Staff at Bell Laboratories, Murray Hill, New Jersey. In 1998 he joined The Chinese University of Hong Kong, where he is now a Professor in the Department of Computer Science & Engineering. Dr. Lyu's research interests include software reliability engineering, distributed systems, fault-tolerant computing, mobile and sensor networks, Web technologies, multimedia information retrieval, data mining, and machine learning. He has published over 400 refereed journal and conference papers in these areas. He has been on the Editorial Board of IEEE Transactions on Knowledge and Data Engineering, IEEE Transactions on Reliability, Journal of Information Science and Engineering, Wiley Software Testing, Verification & Reliability Journal, and IEEE Transactions on Services Computing. Dr. Lyu is an IEEE Fellow, an AAAS Fellow, and received IEEE Reliability Society 2010 Engineer of the Year Award.*

Zhijun Li *received the Dr. Eng. Degree in mechatronics, Shanghai Jiao Tong University, China, in 2002. From 2007 to 2011, he was with the Department of Automation, Shanghai Jiao Tong University, China, as an associate professor. Currently, he is a Professor in College of Automation, South China University of Technology, Guangzhou, China. Prof. Li's current research interests include adaptive/robust control, mobile manipulator, tele-operation system, etc.*